EXPERIMENTAL STUDY OF ENERGY TRASFER RATES IN CO_2 — PROPYL ALCOHOL MIXTURES

A Thesis Submitted
in Partial Fulfilment of the Requirements
for the Degree of
MASTER OF TECHNOLOGY

by
VARANASI SASI DHAR

to the
DEPARTMENT OF CHEMICAL ENGINEERING
INDIAN INSTITUTE OF TECHNOLOGY KANPUR
JUNE, 1977

CERTIFICATE

This is to certify that the present work 'EXPERIMENTAL STUDY OF ENERGY TRANSFER RATES IN CO_2-PROPYL ALCOHOL MIXTURES' has been carried out under my supervision and has not been submitted elsewhere for a degree.

Date: 16th June 1977

Y.V. Chalapati Rao.

[Y.V. Chalapati Rao]
Assistant Professor-
Department of Chemical Engg.
Indian Institute of Technology
Kanpur-208016, India

CHE-1977-M-DHA-EXP

ACKNOWLEDGEMENTS

It is with great pleasure, I express my deep sense of gratitude to Dr. Y.V. Chalapati Rao for his inspiring guidance.

I thank Dr. S.V. Babu and Dr. V. Subba Rao for their incessant encouragement throughout this work.

I am indebted to my friends, M. Tyaga Raju and I.V. Rao for their uninhibited assistance in experimentation and K.K.Rao for lending the subroutine to carry out least square analysis of the experimental data.

The invaluable help rendered in the hour of need by K.M.S. Prasad, deserves special mention.

Thanks are due to R.P. Yadav for his alert attendance during experimentation and B.S. Pandey for his neat typing.

V. Sasidhar

TABLE OF CONTENTS

CHAPTER I

INTRODUCTION

The measurement and prediction of energy transfer rates in gases is a problem of practical importance in the development of new laser systems, chemical kinetics and electrical discharges. During the last decade, chemists and physicists working on the development of powerful, versatile and efficient laser systems have become interested in the details of molecular energy transfer. It is infact the relative rates of energy flow between vibrational modes and among the translational, rotational, and vibrational degrees of freedom which determines the gain, energy, and power characteristics of most molecular gas lasers. A knowledge of the factors affecting energy transfer can often be used to increase the efficiency and power of a given laser system. For example, in the early development of gas laser technology, CO_2 laser power output increased from a level of a few milliwatts for pure CO_2 to several hundred watts for mixtures of CO_2, N_2 and He[1-3]. The enhanced power and efficiency of the mixed gas system are intimately related to the importance of energy transfer between the vibrational modes of CO_2 and N_2 and between the vibrational and translational degrees of freedom of CO_2 and He. At the present time, only a small number of molecules exhibit laser action, but it is reasonable to expect that many new molecular lasers can be developed as knowledge of energy transfer

mechanisms and path ways increases.

Atomic recombination and unimolecular decomposition both depend on the transfer of energy to a vibrational degree of freedom. For example, in the reaction

$$K + HCl \longrightarrow KCl + H$$

at some point in this reaction the H-Cl bond must break. We can expect the reaction to occur with greater probability if the H-Cl bond could be weakened before encountering a K atom. The addition of energy to the vibrational degrees of freedom of HCl constitutes such a weakening because a molecule in an excited vibrational state is closer to the dissociation limit than a molecule in the ground vibrational state. On the other hand, to a good degree of approximation the strength of the H-Cl bond is independent of both translational and rotationan energies. But simply because of this example, we cannot say that translational and rotational energies are not at all important in determining the rate of any chemical reaction. The relative importance of different degrees of freedom (Vibration, Rotation, and Translation) can only be determined by careful consideration of the potential energy surfaces leading from reactants to products[4]. Thus the flow of energy between the various degrees of freedom of a molecule remains a topic of great importance in the development of complete theory of chemical reactivity.

In addition to the practical aspects mentioned above, experimental study of molecular energy flow offers a good test

for energy transfer theories. In this field, theoretical efforts are hampered largely by lack of knowledge of the complete interaction potential between the two colliding molecules. In addition, for polyatomic molecules, the number of energy transfer paths available during a particular collision is so large that theoretical computation of energy transfer cross-sections is not possible without many approximations. Hence experimental data serve as an excellent test for the necessarily approximate treatment of these energy transfer theories.

Shock waves and ultrasonics have long provided the most useful tools for the study of vibration-translation (V-T) energy transfer in gas mixtures. The widely used experimental methods in the study of vibration-vibration (V-V) energy transfer processes are:

1. Ultrasonic and shock wave techniques
2. Optical excitation
3. Flash spectroscopy
4. Monochromatically excited electronic fluorescence
5. Chemical excitation
6. Laser excitation methods.

A brief description of the first five techniques has been presented by Moore[5], and hence their discussion is omitted here. The laser induced fluorescence technique which is employed in the present work is described in detail in Chapter 2.

The vibration-vibration (V-V) energy transfer processes can be conveniently studied by creating a non-equilibrium population among the vibrational energy levels and subsequent observation of the rate at which they relax towards equilibrium. Lasers are the best source for producing such non-equilibrium populations, because of large power density available in a frequency width small compared with the molecular absorption linewidth[6]. In this work, the energy transfer rates from the asymmetric stretching mode of CO_2 to n-Propyl alcohol and iso-propyl alcohol are studied. A 10.6μ Q-switched CO_2 laser is used to excite $(00^0 1)$ mode (asymmetric stretching mode) of CO_2 molecule. The rate of decay of the molecules in this level, due to collisions with CO_2 and added alcohol molecules, is then followed by observing the intensity of the $(00^0 1) \rightarrow (00^0 0)$ spantaneous emission in CO_2 as a function of time. The energy transfer cross-sections are measured over the temperature range 303-514^{0}K for 3 different compositions of the mixtures. The observed negative temperature dependence and large magnitudes of energy transfer rates suggest that the energy transfer processes are caused by long range forces. A detailed description of the experimental set up used in the present work is also included in Chapter 2. The relevant theories to predict the energy transfer probabilities are briefly mentioned in Chapter 3. Chapter 4 presents the experimental results and discussion. Lastly the conclusions arrived at are mentioned in Chapter 5.

CHAPTER 2

EXPERIMENTAL TECHNIQUE AND SET UP

The vibration-vibration (V-V) energy transfer processes are best studied by creating a non-equilibrium distribution among the vibrational levels of the molecule and subsequent observation of the rate at which they decay towards the equilibrium distribution. The laser induced fluorescence method has several advantages over the conventional methods of ultrasonic absorption and shock waves for the measurement of these rates. In general, any laser which operates on a vibrational transition permits that transition to be excited in a gas sample which is subjected to the laser radiation. Hence the initial excited level of the gas is known in the laser excited fluorescence technique. The shock tube and ultrasonic absorption techniques are limited by the fact that excitation must go through the translational degrees of freedom. In these techniques, it is not possible to uniquely specify the initial excited level and the analysis of the data in polyatomic molecules is generally complicated. The narrow pulse widths and large power densities available in laser radiation are extremely useful in the study of energy transfer processes in gases and gas mixtures. The only limitation of the laser induced fluorescence technique is that the energy transfer processes can be studied in only those molecules which absorb laser radiation. With the development of new laser systems,

the number of molecules which could be studied will increase.

In the present study $CO_2(00^01)$ level is excited by a 10.6μ and 9.6μ Q-switched CO_2 laser pulse. During the pulse duration the (10^00), $(02^00) \dashrightarrow (00^01)$ transition in CO_2 present in the sample is nearly saturated. The application of an intense laser pulse thus leads to a population in (00^01) level of CO_2 that is in excess of that at equilibrium. In the time between two laser pulses, this level (00^01) decays to equilibrium with a time constant, τ, called the relaxation time. Since (00^01) level is optically connected to the ground state, spantaneous emission occurs at 4.3μ. The intensity of this fluorescence is proportional to the excess number of molecules in the (00^01) level and the rate at which the populations attains its equilibrium value can be studied by monitoring the rate of decay of the intensity of the fluorescence signal.

The excess population in the (00^01) level of CO_2 is removed by all the following three independent processes simultaneously.

(i) Collisions with other molecules

(ii) Spontaneous emission of radiation

(iii) Diffusion and subsequent deactivation by collisions with the walls of container.

Hence the observed time constant (τ) can be expressed as

$$\left(\frac{1}{\tau}\right)_{\text{observed}} = \left(\frac{1}{\tau}\right)_{\text{collisions}} + \left(\frac{1}{\tau}\right)_{\text{radiation}} + \left(\frac{1}{\tau}\right)_{\text{diffusion}} \qquad (2.1)$$

Of the above processes, the collisional deactivation rate $\left(\frac{1}{\tau}\right)_{\text{coll.}}$ is directly proportional to the pressure and the diffusion rate to the walls, $\left(\frac{1}{\tau}\right)_{\text{diff.}}$ varies inversely as the pressure. The radiative decay rate $\left(\frac{1}{\tau}\right)_{\text{rad.}}$ is independent of the pressure. In the present experiments, the pressures are high enough for the diffusion rate to be negligible. Hence a plot of $\left(\frac{1}{\tau}\right)_{\text{obs}}$ vs pressure gives a straight line. The slope of this line $(P\tau)^{-1}_{\text{coll.}} = K_{\text{obs}}$ gives the collisional deactivation rate constant.

The observed rate constant K_{obs} is composed of the deactivation by collisions with other CO_2 molecules and by collisions with M (M being either ISO - or Normal - propyl alcohol molecules). Hence by studying the dependence of the K_{obs} values on the composition of the gas mixture, it is possible to obtain the deactivation rate $K_{CO_2\text{-}M}$ solely by collisions with M which is a direct measure of the rate of energy transfer from $CO_2(00^0 1)$ to M. The temperature dependence of this $K_{CO_2\text{-}M}$ gives us information about the nature of intermolecular forces which cause the energy transfer. If the rate constants increase with temperature, short range forces are expected to be dominant[7,8]. On the other hand, if the system shows negative temperature dependence long range forces are supposed to be controlling the energy transfer process[9,10].

The experimental data on energy transfer is generally reported in terms of the deactivation rate constant K_{CO_2-M}, the collision cross-section for energy transfer σ, and the energy transfer probability per collision P. These are inter-related as follows:

$$\sigma = (K/nv) \qquad (2.2)$$

$$P = \left(\frac{\sigma}{\pi d^2}\right) \qquad (2.3)$$

where n - number density of molecules

v - average relative velocity of the colliding pair and

d - average diameter of the colliding pair

Thus for CO_2-M collisions,

$$d = \tfrac{1}{2}[d(CO_2) + d(M)] \qquad (2.4)$$

Experimental Set-up:

The experimental set-up is similar to that described previously by Rao[11] except that the test cell which can be used upto 1000°K. A block diagram of the experimental set-up is shown in Figure 1. In brief the laser consists of a water cooled discharge tube, 25 mm I.D., 4 meter length of pyrex glass. One end is sealed at Brewster's angle with a Harshaw polished NaCl window, 60 mm diameter and 5 mm thickness. The other end is closed with a 10 m radius of curvature gold coated output mirror with a 6 mm diameter central hole. This hole is closed with a NaCl window. A mixture of CO_2:Nitrogen; Helium in the ratio of 1:1.5:1 is pumped through the tube at a pressure of about 15 Torr with a 160 lit/min mechanical pump. The mixture

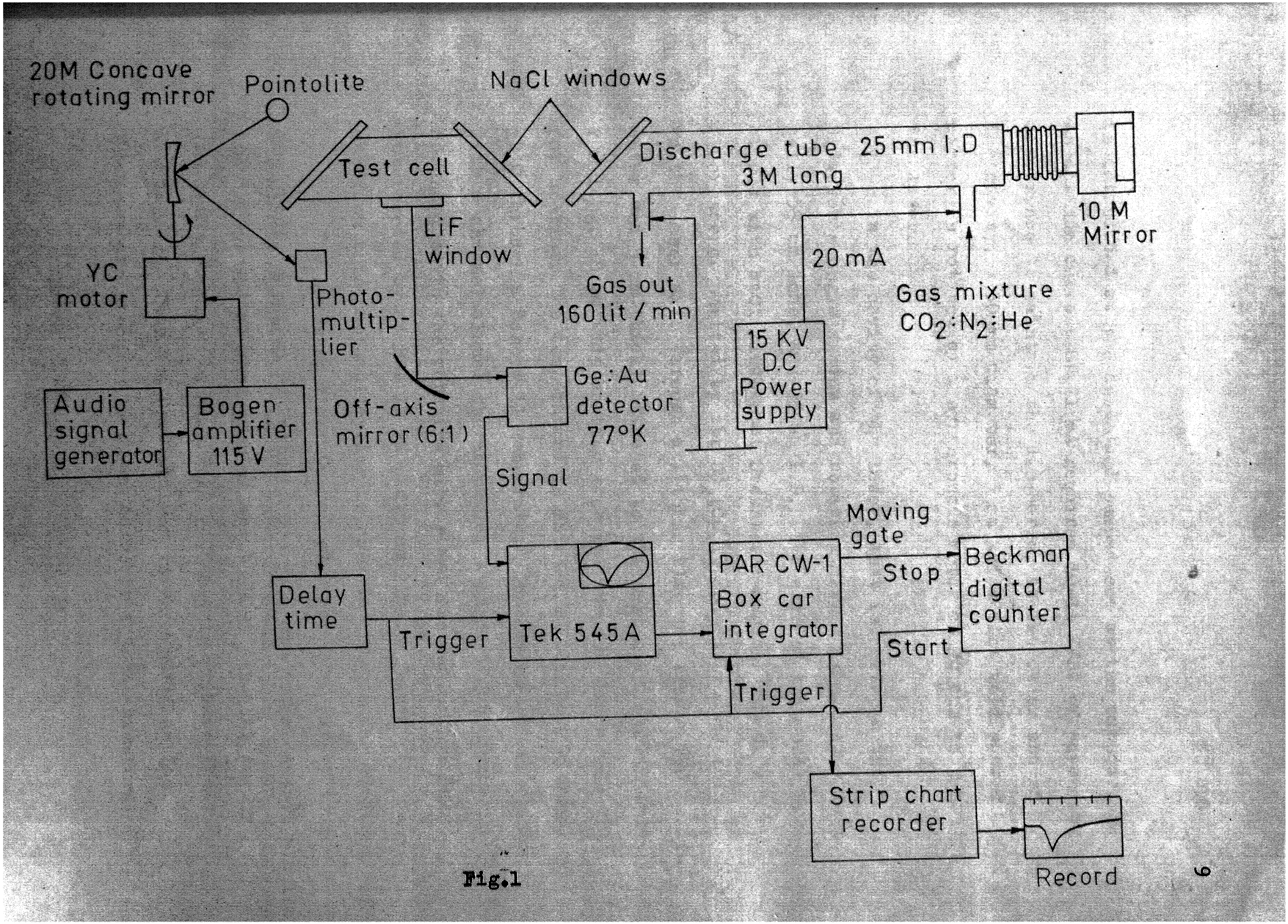
20M Concave rotating mirror
Pointolite
NaCl windows
Test cell
Discharge tube 25 mm I.D
3M long
10 M Mirror
LiF window
YC motor
Photo-multip-lier
Gas out 160 lit / min
20 mA
Gas mixture CO_2:N_2:He
15 KV D.C Power supply
Audio signal generator
Bogen amplifier 115 V
Off-axis mirror (6:1)
Ge:Au detector 77°K
Signal
Moving gate
Delay time
Trigger
Tek 545A
PAR CW-1 Box car integrator
Stop
Beckman digital counter
Start
Trigger
Strip chart recorder
Record

Fig.1

is introduced at the anode and pumped out at the cathode. An optimum current of 21 mA required 10-11 KVDC of potential difference to maintain the discharge. At the other end of the cavity, a 50 mm diameter, 5 mm thick flat gold coated mirror is rotated by a synchronous motor at 70 cps to Q-switch the laser.

In the cavity of the laser, that is, between the Brewster's angle window and rotating mirror is placed a test cell, 35 cm long, and 25 mm I.D. The ends of this cell are closed with NaCl windows at Brewster's angle. The 4.3μ fluorescence emitted by the $CO_2(00^o1)$ mode is viewed normal to the laser axis through a lithium fluoride window (50 mm diameter and 5 mm thick) attached to the test cell. A 400 watt, 2 m long, 18 mm wide heating tape is wound on the sample cell for heating. The temperature is maintained constant within $\pm 2^oC$ through a Honeywell Temperature Controller and is measured with a chromel-alumel thermocouple. A point light source is focussed on to the rotating mirror and its reflection is intercepted by an RCA 1P 28 photo multiplier tube. The output from this photomultiplier is used to trigger the electronics.

The gases used are CO_2 of 99.8 per cent purity (Bone-dry grade, supplied by Matheson Gas Co.) and normal-propyl alcohol and iso-propyl alcohol each of about 99.95 per cent purity (AR grade, supplied by High Purity Chemicals Private Limited, New Delhi). They are used without further purification. Mixtures are prepared in glass bulbs at a total pressure of

about 400 Torr which are thoroughly evacuated to 10^{-4} Torr for a few hours before mixing. They are left for atleast for 24 hours for complete mixing before the sample is withdrawn for fluorescence studies. The composition of the gas mixture is estimated from the partial pressures.

The 4.3μ fluorescence viewed through a LiF window, which blocks the radiation above 7μ, is focussed onto Ge:Au detector (SBRC) by an off-axis mirror (6:1). The detector is cooled to 77°K and loaded with 10 kilo-ohms. The output voltage from the detector is displaced on TeK-549 oscilloscope provided with a 1A7A plug-in unit. A typical oscillogram is shown in Figure 2. The vertical amplifier output from the oscilloscope is fed to the PAR CW-1 Box-car integrator, to improve the signal to noise ratio. The usual integration times are 20 minutes, with a time constant of 0.1 msec and gate width of 1 μ sec.

The output from the box-car is recorded on a Bausch-Lomb Vom-6 strip chart recorder. The response time of the detector with the associated electronics is approximately 3 μ sec A sample is used to obtain a couple of records and discarded. A fresh sample is taken for subsequent runs. The studies are performed over a pressure range of 2-28 Torr. A silicone oil manometer is used to measure the gas pressure in the test cell. The maximum pressure in the cell is limited by the response time of the detector with the associated electronics and the lower pressures by the diffusion to the cell walls.

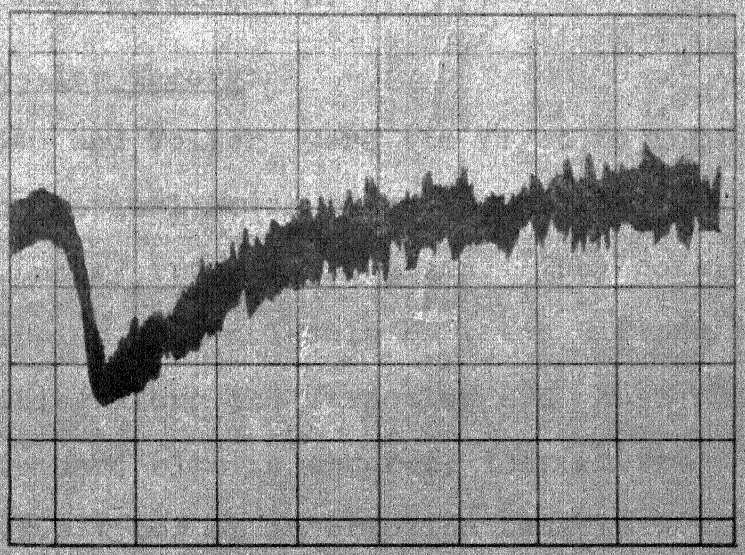

Fig. 8 - Typical oscillogram of the fluorescence signal.

CHAPTER 3

ENERGY TRANSFER THEORIES

The various theories of energy transfer attempt to estimate the probability that a molecule undergoes a transition from one vibrational state to the other due to intermolecular interaction during collision.

Landau and Teller Theory:

Landau and Teller[7] were the first to formulate a classical theoretical model to understand the mechanism of vibrational energy transfer in gases. They considered the head-on collision of a molecule BC (atom C fixed in space) with A, A approaching along the direction BC. When the colliding molecules are hard elastic spheres, they interact upon direct collision. Two types of interaction between B and A are possible. They are (1) adiabatic and (2) non-adiabatic collisions. In the case of adiabatic collisions the efficiency of energy transfer is zero and in the case of non-adiabatic collisions the energy transfer efficiency is very high. Landau and Teller pointed out that the probability of energy transfer depends on the ratio of the period of vibration to the time of interaction. The ratio is given by $(\frac{l\nu}{V})$ where ν is the vibration frequency, l is the characteristic length and V is the relative velocity of the colliding atom (A). From this, they concluded that only short range forces are effective in producing transition. Since the repulsive intermolecular forces have shorter range than the

attractive ones, only the repulsive forces need to be considered.

Landau and Teller assumed an exponential interaction law and deduced the transition probability function ($\frac{1}{Z}$), which is given by

$$\frac{1}{Z} = \frac{1}{Z'_o} \sqrt{\frac{2\pi}{3}} \left(\frac{\varepsilon'}{kT}\right)^{1/6} \exp\left[-\frac{3}{2}\left(\frac{\varepsilon'}{kT}\right)^{1/3}\right] \qquad (3.1)$$

Thus $k \alpha \exp(-CT^{-1/3})$. Hence a plot of $\ln k$ vs $T^{-1/3}$ should yield a straight line.

Schwartz, Slawsky and Herzfeld (SSH) Theory:

Schwartz, Slawsky and Herzfeld[8] extended the theory to chemically non-reactive gas mixtures and to gas molecules with several normal vibrational modes. They considered the molecules to be rotationless and approach each other along a straight line. They handled the problem with three dimensional quantum mechanical treatment and found that

$$P \sim \exp\left[-3(\Delta E^2 \mu \pi^2/2 \alpha^2 \bar{n}^2 kT)^{1/3}\right] \qquad (3.2)$$

which means that P increases with increasing T, and decreases with increasing (ΔE). In this expression, α is the relative approach velocity, μ is the reduced mass and k is the Boltzmann constant. The temperature dependence and the magnitude of the energy transfer probabilities predicted by the SSH theory are consistent with the available experimental data in many systems in the case of vibration-translation (V-T) energy transfer where large amounts of energy are exchanged with translation.

Sharma-Brau Theory:

The theories of Landau and Teller and SSH considered short range forces and showed that the probability for vibrational exchange increased with temperature. However the experiments of Rosser, Wood and Gerry[12] showed a negative temperature dependence below 1000°K, that is, probability of energy exchange decreasing with temperature in the vibration-vibration transfer between CO_2 ($00^0 1$) and N_2 (v=0). In this energy exchange, the energy deficit is only 18 cm^{-1}. Such processes for which the energy mismatch is very small are said to be near-resonant processes.

Sharma and Brau[9,10] explained this negative temperature dependence of vibrational energy exchange probability by considering the long range dipole-quadrapole interaction between these molecules. The calculations based on Sharma and Brau theory were in excellent agreement with the experimentally[9,13] observed temperature dependence (T^{-1}) of the near resonant vibrational relaxation processes.

According to Sharma and Brau, the probability that vibrational energy transfer will occur during a collision described by a classical trajectory R(t) may be written as

$$P = \left(\frac{1}{\hbar^2} \left| \int_{-\infty}^{\infty} e^{iwt} \langle f | \; V[R(t)] \; | i \rangle \, dt \right|^2 \right) \quad (3.4)$$

Here $\hbar w$ is the amount of energy transferred to translation (the net change in vibrational energy during the collision),

$|i\rangle$ and $|f\rangle$ are the initial and final vibration-rotation wave functions, and V[R(t)] is the intermolecular potential function including its dependence on all the vibrational, rotational co-ordinates. The long range parts of intermolecular potential, may give significant probabilities for nearly resonant energy transfers but are rapidly averaged to zero as w increases.

—

CHAPTER 4

EXPERIMENTAL RESULTS AND DISCUSSION

Using the laser induced fluorescence technique, the deactivation of the $CO_2(00^0 1)$ mode in collisions with n-propyl alcohol and iso-propyl alcohol is studied. The temperature range studied is 303-514^{0}K for n-propyl alcohol and 303-512^{0}K for iso-propyl alcohol. At higher temperatures, the reproducibility of the data is checked by the following method to make sure that no dissociation of the alcohols occurred. The relaxation time τ of a sample at a given pressure P is first measured at room temperature and the temperature of the sample is then raised to the desired value and maintained there for an hour. Then the sample is cooled back to room temperature and the pressure and relaxation time are again measured. These measurements agreed within the experimental error in the temperature ranges mentioned above confirming that no appreciable dissociation or association of the sample occurred in the temperature range.

The rates of energy transfer are studied as a function of composition of the gas mixture at each temperature and it is observed that the rates increased linearly with increasing composition of the collision partner, in the composition range studied. The maximum composition of the mixtures with which experiments are carried out, are limited by the time constant

of the detector and the associated electronics. The maximum compositions studied are 3.7 per cent in the case of normal-propyl alcohol and 4.1 per cent in the case of iso-propyl alcohol. The rate constant for deactivation of $CO_2(00^0 1)$ due to collisions with alcohol molecules is obtained by extrapolating the measured rates to 100 per cent alcohol. In both the systems studied, the rate constants are found to decrease with increasing temperature. The large magnitudes and the negative temperature dependence of the rate constants suggest that near-resonant processes are responsible for the deactivation of $CO_2(00^0 1)$ in both systems. As discussed earlier, long range intermolecular forces are expected to be dominant in causing energy transfer in such processes.

Carbon Dioxide - Normal Propyl Alcohol:

The fluorescence from $CO_2(00^0 1)$ at 4.3μ exhibited a single exponential decay with a time constant τ for all the mixtures studied for this system. A typical fluorescence decay curve (1 per cent n-propyl alcohol, at a pressure of 17.0 Torr and 437°K) is shown in Figure 3. A semi-log plot of the intensity of the fluorescence versus time, shown in Figure 4, resulted in a straight line with slope $\tau^{-1} = (28.5 \text{msec}^{-1})$. The experiment is conducted at about ten different pressures in the range 4.4 to 28 Torr and at each pressure the value of τ^{-1} is obtained. It can be seen from equation (2.1) that as long as the radiative and diffusional contributions to the

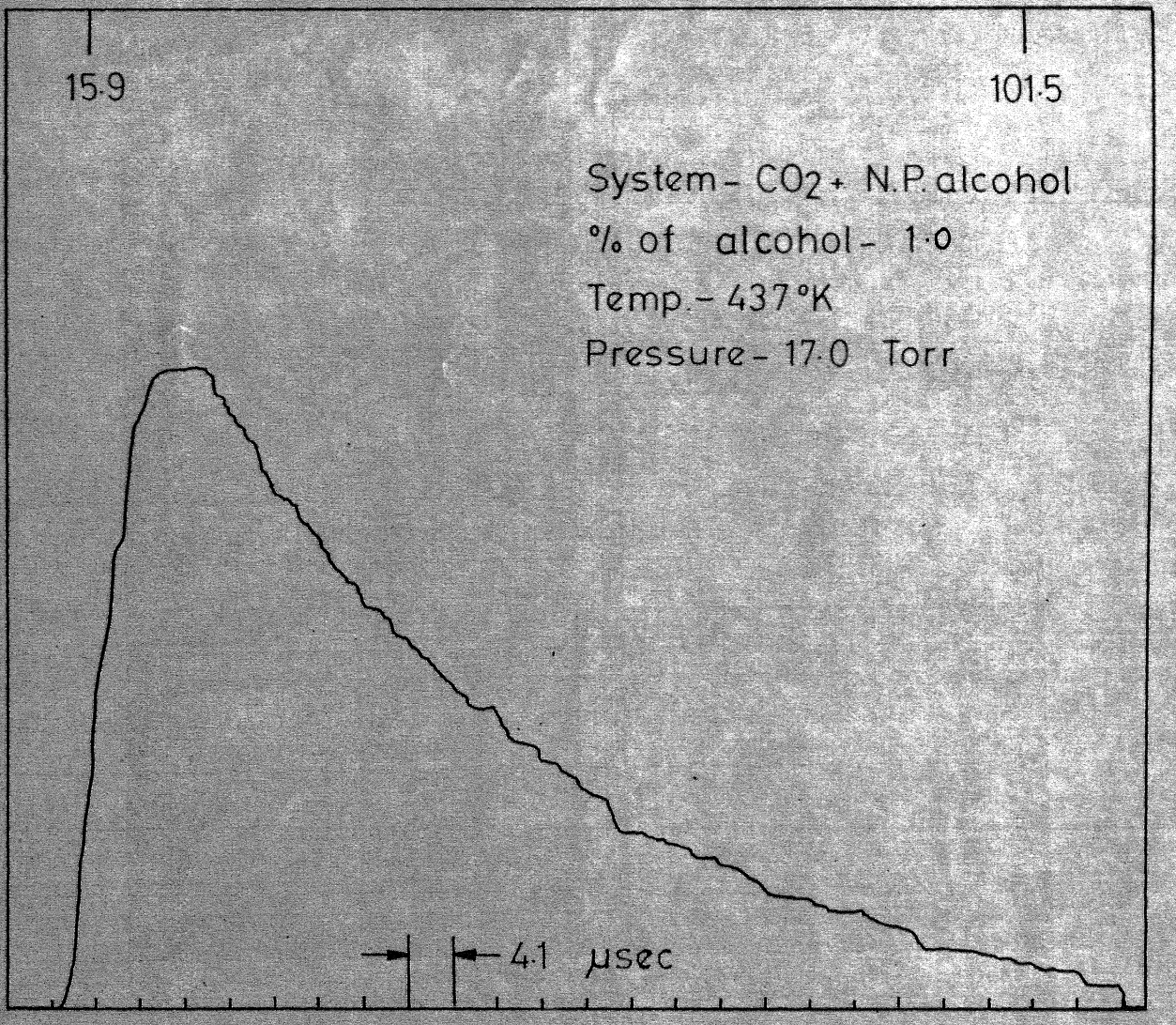

Fig. 3 - Typical fluorescence decay curve.

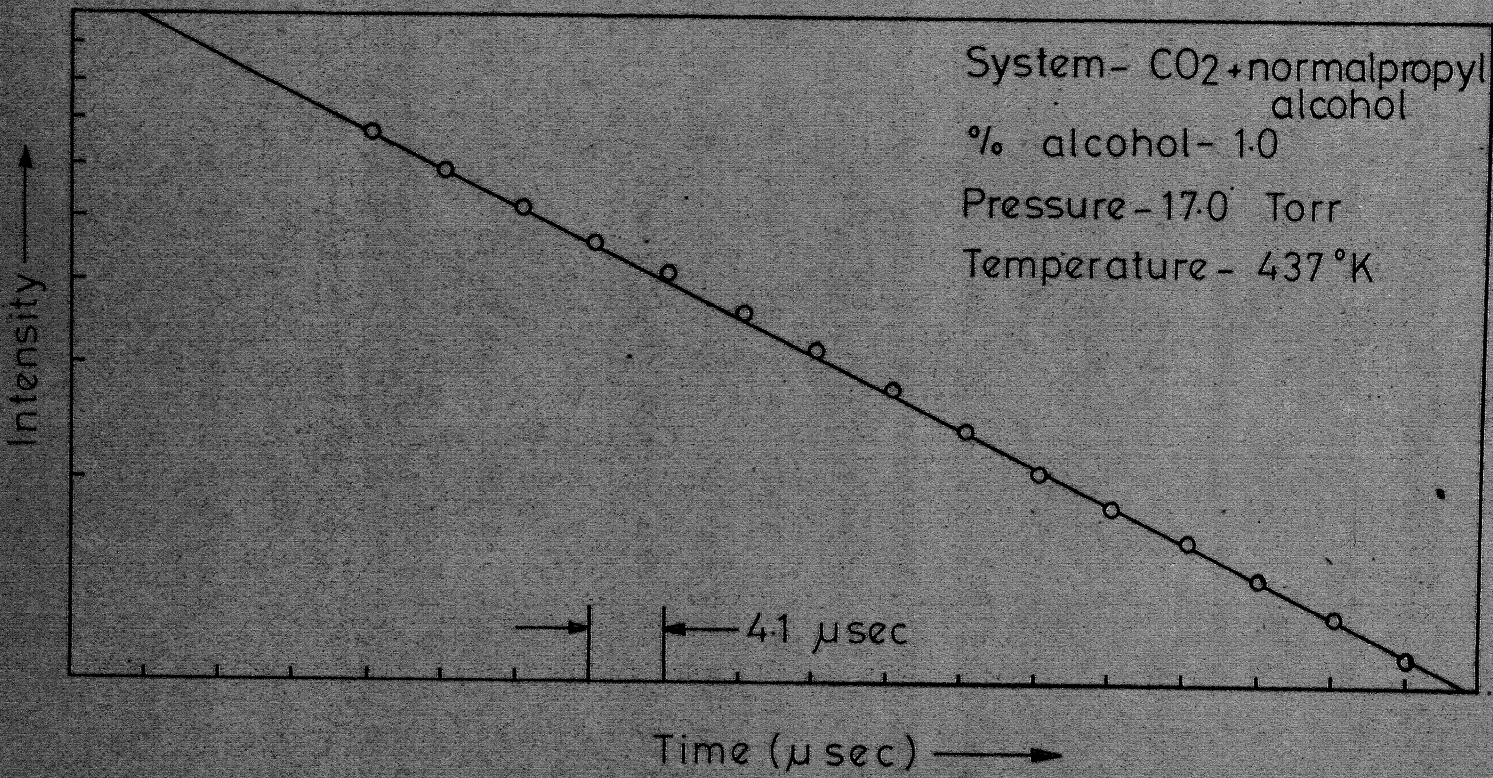

Fig. 4 - Semi-log plot of I vs. t.

deactivation rate are negligible, the observed τ^{-1} represents only the collisional deactivation rate of $CO_2(00^01)$. In Figure 5, τ^{-1} is plotted against pressure P and it can be observed from the figure that $(\tau)^{-1}$ is proportional to pressure P indicating that only bimolecular collisions are dominant in the pressure range studied. A least square analysis of the data of τ^{-1} versus pressure is made to get $(P\tau)^{-1} = K_{obs}$ values with the corresponding standard deviation. The values of $(P\tau)^{-1}$ are thus obtained for three different mixtures of CO_2 and normal-propyl alcohol (1.0 per cent, 2.0 per cent and 3.7 per cent n-propyl alcohol) at 4 temperatures, 514°K, 437°K, 371°K and 305.5°K (room temperature). A plot of $(P\tau)^{-1}$ as a function of X_M (mole fraction of normal-propyl alcohol in the binary mixture) is shown in Figure 6 and the linearity of the plots suggests that

$$K_{obs} = K_{CO_2-CO_2} X_{CO_2} + K_{CO_2-M} X_M \qquad (4.1)$$

where M = normal-propyl alcohol

In the above expression, $K_{CO_2-CO_2}$ represents the rate constant for the deactivation of $CO_2(00^01)$ in collisions with carbon-dioxide molecules only and K_{CO_2-M} is the rate constant for energy transfer in collisions with normal-propyl alcohol only. The rate constant K_{CO_2-M} is then obtained by extrapolating the K_{obs} values. Once again a least square fit of K_{obs} versus X_M is made to get K_{CO_2-M} with error limits. The values of

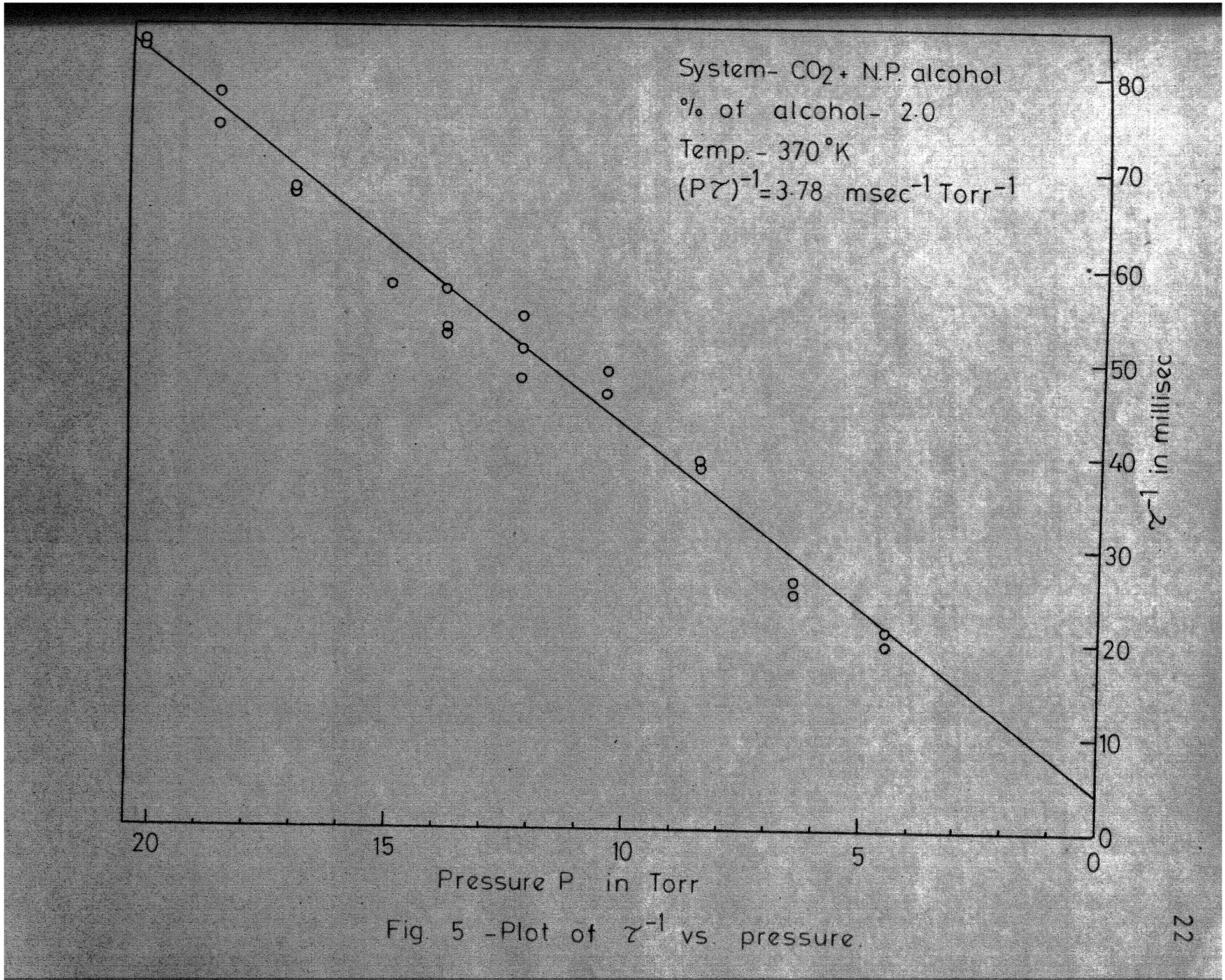

Fig. 5 -Plot of τ^{-1} vs. pressure.

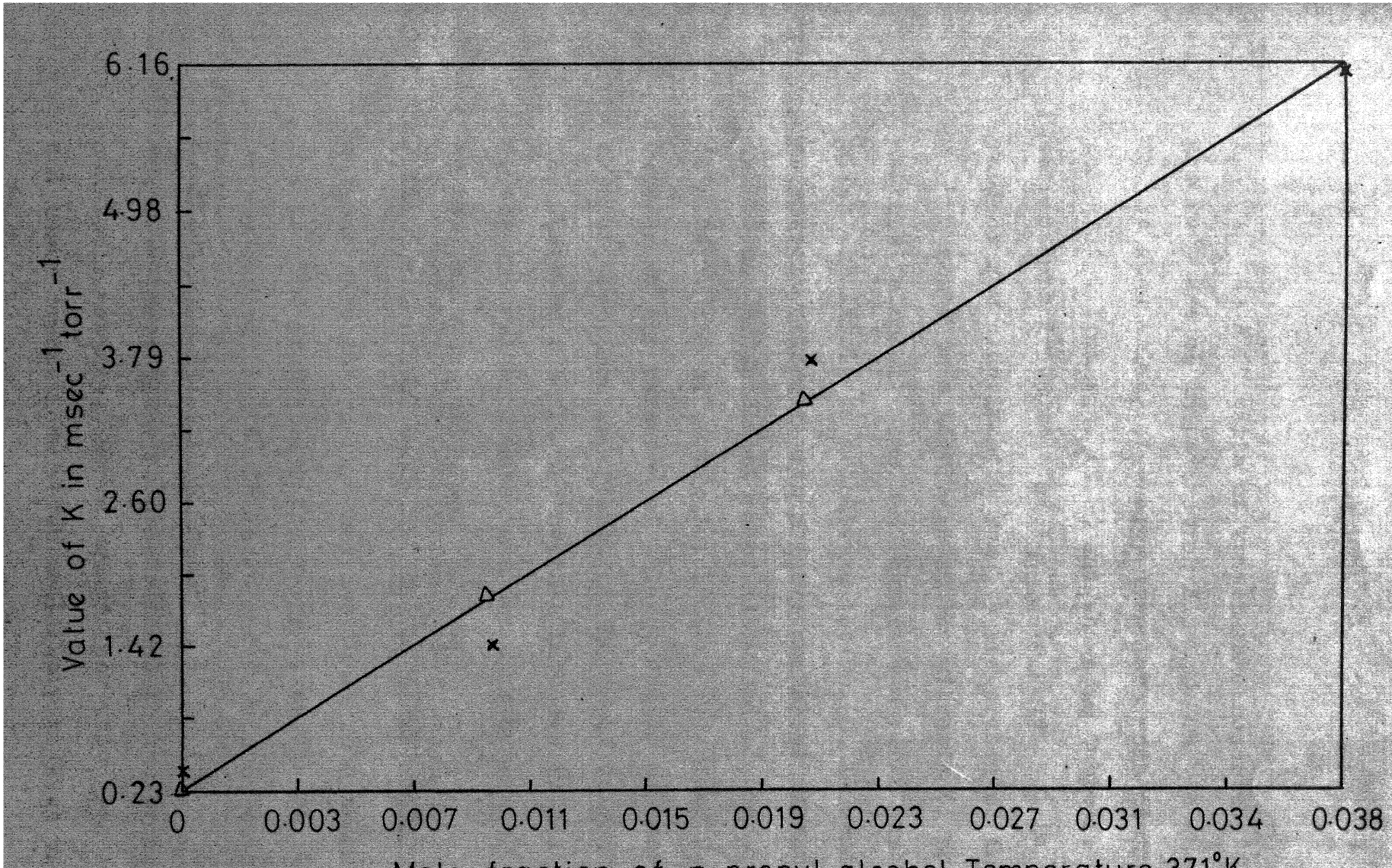

Fig. 6 - Dependence of $(P\gamma)^{-1}$ on $X_{N.P.}$ alcohol.

$K_{CO_2-CO_2}$ as a function of temperature reported [11,13] earlier are made use of in estimating K_{CO_2-M}. The rate constants and the related values of energy transfer cross-sections are calculated from eqn. (2.2) and shown in Table I. The temperature dependence of K_{CO_2-M} is presented in Figure 7. The rest of the experimental results are presented in Tables 2-5.

Based on a knowledge of the vibrational spectra of n-propyl alcohol[14] one can enumerate a large number of processes which are likely to deactivate the $CO_2(00^0 1)$ mode. For a polyatomic molecule with a large number of vibrational levels including the fundamental, overtone and combination bands, the identification of particular process is rather difficult. Because of the presence of a large number of energy levels, several processes contribute to the deactivation of $CO_2(00^0 1)$. The observed rate is the overall rate due to all these processes. Of the several processes, one can eliminate many of them based on the following criteria.

1. Energy Deficit: The probability of energy transfer is maximum when the energy that has to go into translation is very small. The probability for energy transfer is very small if energy deficit (ΔE) is large and such processes can be ignored.

2. Transition Multi-Pole Moments: It is known that the energy transfer probability is proportional to the product of transition multipole moments. Hence transitions which are infrared inactive and those transitions which are likely to have very little

TABLE 1: RATE CONSTANTS AND CROSS SECTIONS OF ENERGY TRANSFER FROM $CO_2(00^01)$ TO N-PROPYL ALCOHOL

Temp. in ^oK	Mole Fraction of n-Propyl alcohol	$(P\tau)^{-1}$ m sec^{-1}x $torr^{-1}$	K sec^{-1}x $torr^{-1}$	σ^a $(\AA)^2$
305.5	0.010	2.11 ± 0.15[b]		
	0.021	5.56 ± 0.23	(164.48±28.65)x10^3	1.038
	0.038	6.39 ± 0.96		
371.0	0.010	1.42 ± 0.13		
	0.021	3.77 ± 0.13	(154.46±9.56)x10^3	1.074
	0.038	6.11 ± 0.56		
437.0	0.010	1.22 ± 0.08		
	0.021	2.75 ± 0.18	(70.73 ±12.34) x10^3	0.534
	0.038	3.12 ± 0.24		
514.0	0.010	1.29 ± 0.07		
	0.021	1.86 ± 0.13	(53.05±2.07)x10^3	0.434
	0.038	2.89 ± 0.23		

[a] The cross-sections σ are calculated according to eq.(2.2).
[b] The error limits correspond to 95 per cent confidence limits

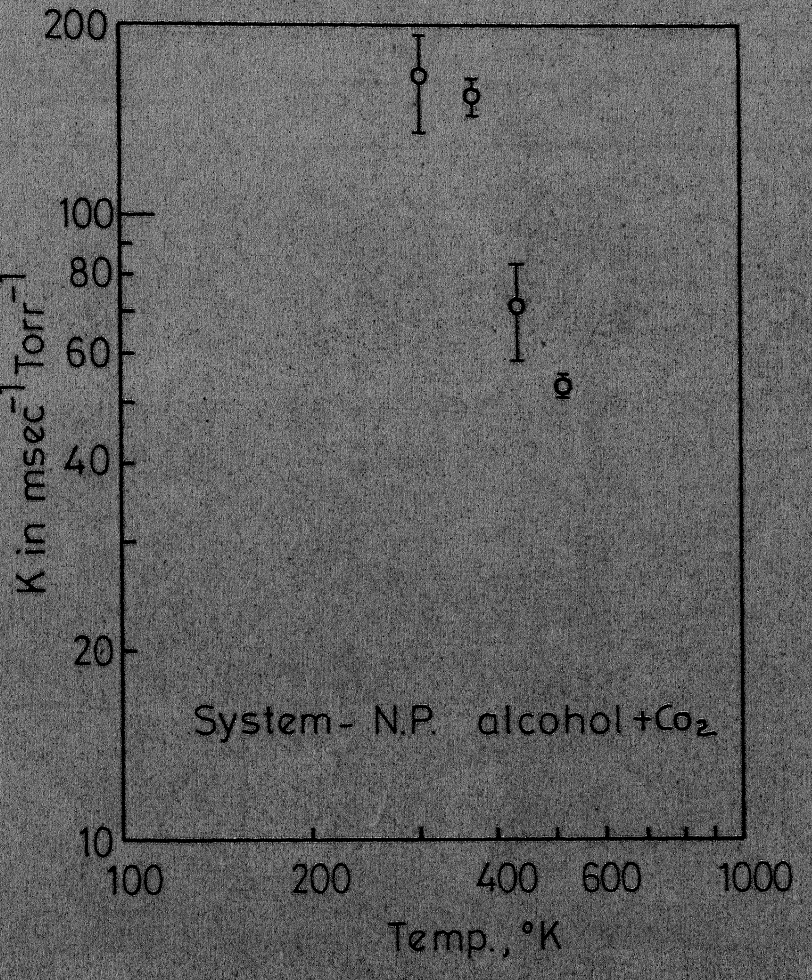

Fig. 7 -Temperature dependence of K.
(ln K vs. ln T)

TABLE 2

Temperature = 514°K System: Carbondioxide - n-Propyl Alcohol

Pressure (P) in Torr; τ^{-1} in $msec^{-1}$; X-mole fraction of Alcohol

X = 0.038		X = 0.021		X = 0.010	
P	τ^{-1}	P	τ^{-1}	P	τ^{-1}
4.0	17.57	4.1	18.45	3.3	10.21
4.0	19.54	4.1	19.26	3.3	11.17
5.6	23.00	5.7	24.00	4.9	14.66
5.6	25.03	5.7	21.32	4.9	13.98
7.4	34.39	7.4	25.42	7.0	16.95
7.4	30.9	7.4	24.10	7.0	17.34
9.4	22.43	7.4	24.34	7.0	19.05
9.4	28.13	10.3	28.73	8.8	22.02
11.1	37.29	10.3	28.43	8.8	21.09
11.1	30.70	10.3	28.97	11.1	20.66
11.1	50.30	12.2	34.30	11.1	25.39
12.6	40.36	12.2	39.61	11.1	22.63
12.6	55.72	12.2	39.15	13.8	28.55
12.6	52.10	13.4	38.07	13.8	27.69
14.2	51.21	13.4	41.53	16.1	32.11
14.2	53.25	13.4	39.50	16.1	30.80
16.3	48.11	15.2	43.04	16.1	30.80
16.3	51.25	15.2	40.24	19.7	35.66
16.3	48.55	17.6	46.85	19.7	37.40
18.2	72.59	17.6	51.17	23.0	40.33
18.2	67.19	17.6	45.74	23.0	34.17
21.4	69.04	17.6	47.70	27.0	44.45
21.4	61.70	19.2	54.18	27.0	36.77
21.4	71.01	19.2	50.33		
		23.0	52.29		
		23.0	51.95		
		23.0	43.54		
$(P\tau)^{-1}=(2.89\pm0.23)$ $msec^{-1}Torr^{-1}$		$(P\tau)^{-1}=(1.86\pm0.13)$ $msec^{-1}Torr^{-1}$		$(P\tau)^{-1}=(1.29\pm0.07)$ $msec^{-1}Torr^{-1}$	

TABLE 3

Temperature = 437°K System: Carbon Dioxide-n-propyl Alcohol

Pressure (P) in Torr; $(\tau)^{-1}$ in $msec^{-1}$; X-mole fraction of alcohol

X=0.038		X=0.021		X=0.010	
P	τ^{-1}	P	τ^{-1}	P	τ^{-1}
2.8	21.83	3.4	15.21	4.4	18.06
2.8	21.58	3.4	15.22	4.4	15.86
3.9	25.55	5.0	20.34	4.4	16.79
3.9	35.37	5.0	18.87	6.6	19.57
5.4	36.35	6.7	20.80	6.6	20.49
5.4	32.67	6.7	20.78	8.4	20.33
7.0	38.37	8.4	30.90	8.4	20.07
7.0	46.57	8.4	29.30	10.5	25.02
8.6	56.11	10.6	34.03	10.5	26.07
8.6	51.28	10.6	32.47	12.7	25.34
10.6	56.23	12.6	37.75	12.7	25.75
10.6	62.83	12.6	47.80	14.2	30.85
10.6	57.83	15.4	42.94	14.2	29.21
12.2	53.63	15.4	64.60	17.1	32.05
12.2	55.79	18.9	63.22	17.1	28.50
13.6	58.11	18.9	48.13	20.6	35.72
13.6	56.20	22.7	78.29	20.6	33.59
17.0	76.40	22.7	56.97	25.5	41.81
17.0	62.97	25.5	83.50	25.5	34.59
19.3	81.66	25.5	73.22	25.5	40.43
19.3	75.21	25.5	71.66	28.0	46.79
				28.0	55.27

$(P\tau)^{-1} = (3.12 \pm 0.23)$ $msec^{-1}Torr^{-1}$ $(P\tau)^{-1} = (2.75 \pm 0.18)$ $msec^{-1}Torr^{-1}$ $(P\tau)^{-1} = (1.21 \pm 0.08)$ $msec^{-1}Torr^{-1}$

TABLE 4

Temperature=371°K System: Carbon dioxide-n-propyl Alcohol

Pressure (P) in Torr; $(\tau)^{-1}$ in $msec^{-1}$; X-mole fraction of alcohol

X=0.038		X=0.021		X=0.010	
P	τ^{-1}	P	τ^{-1}	P	τ^{-1}
3.2	23.70	4.5	20.71	4.6	12.75
3.2	22.11	4.5	19.60	4.6	13.03
4.2	29.12	6.4	26.33	4.6	13.03
4.2	29.93	6.4	24.90	6.4	14.66
6.4	44.27	8.4	38.85	6.4	14.66
6.4	44.27	8.4	38.51	7.9	15.10
7.7	54.69	10.4	48.79	7.9	13.67
7.7	45.36	10.4	46.42	9.8	17.49
9.8	79.46	12.2	54.58	9.8	17.99
9.8	65.30	12.2	50.99	11.3	20.50
11.3	94.00	12.2	47.96	11.3	21.83
11.3	88.27	13.8	57.42	13.3	29.16
11.3	90.52	13.8	53.11	13.3	27.13
11.3	63.90	13.8	52.55	16.2	35.73
12.9	82.99	15.0	57.68	16.2	41.22
12.9	79.36	15.0	57.81	19.2	26.09
14.8	84.64	17.0	67.11	19.2	26.76
14.8	85.200	17.0	67.32	21.6	34.31
		18.6	69.05	21.6	38.70
		18.6	77.46	25.7	40.85
		20.2	82.62	25.7	42.75
		20.2	83.03		
$(P\tau)^{-1}=(6.10\pm0.56)$ $msec^{-1}Torr^{-1}$		$(P\tau)^{-1}=(3.77\pm0.13)$ $msec^{-1}Torr^{-1}$		$(P\tau)^{-1}=(1.41\pm0.13)$ $msec^{-1}Torr^{-1}$	

TABLE 5

Temperature=305.5°K- System:Carbondioxide-n-Propyl Alcohol
Pressure(P) in Torr; $(\tau)^{-1}$ in $msec^{-1}$; X-mole fraction of alcohol

X=0.038		X=0.021		X=0.010	
P	τ^{-1}	P	τ^{-1}	P	τ^{-1}
3.9	66.73	3.1	27.59	4.6	32.93
3.9	63.59	3.1	31.19	4.6	27.17
5.5	67.45	4.8	33.91	6.4	30.05
5.5	77.06	4.8	31.30	6.4	26.15
6.7	76.06	4.8	30.61	7.7	29.16
6.7	93.41	6.4	45.16	7.7	28.98
8.2	89.10	6.4	49.16	10.0	29.69
8.2	111.99	7.8	57.28	10.0	31.65
9.0	81.44	7.8	48.52	11.8	36.07
9.0	79.39	9.4	71.71	11.8	36.83
10.1	102.19	9.4	56.41	14.2	43.22
10.1	114.02	9.9	55.19	14.2	40.05
10.1	99.03	9.9	58.46	15.9	50.02
12.4	112.34	11.0	60.04	15.9	44.26
12.4	107.70	11.0	60.00	15.9	55.02
13.0	97.99	13.1	82.06	17.7	54.93
13.0	89.34	13.1	80.70	17.7	56.67
14.1	111.69	14.8	98.02	19.6	50.05
14.1	120.99	14.8	83.72	19.6	54.65
16.4	147.20	14.8	84.17	22.2	63.02
16.4	191.88	16.4	98.23	22.2	65.50
		16.4	97.61		
		22.7	147.49		
		22.7	128.15		

$(P\tau)^{-1}=(6.39\pm0.96)$ $msec^{-1}Torr^{-1}$ $(P\tau)^{-1}=(5.56\pm0.23)$ $msec^{-1}Torr^{-1}$ $(P\tau)^{-1}=(2.11\pm 0.16)$ $msec^{-1}Torr^{-1}$

transition multipole moments can be ignored.

3. Energy Level Population: Since the molecules are distributed among the various energy levels according to Boltzmann distribution, the number of molecules in the higher excited energy levels will be very small. Therefore, it is enough to consider the collision partners in the ground state or in the low lying vibrational energy levels for the deactivation of $CO_2(00^01)$.

4. Quantum Number Changes: The probability of transition from the ground state to a fundamental level is two orders of magnitude larger than that of transition from ground state to overtone. Hence processes involving fundamental levels are preferred over those involving overtones for the same amount of energy deficit.

Based on the above criteria the following processes are likely to be responsible in the deactivation of $CO_2(00^01)$.

$$CO_2(00^01) + M = CO_2(10^00) + M\ (\tilde{\nu} = 971\ cm^{-1}) + \Delta E = -10\ cm^{-1}$$

$$CO_2(00^01) + M = CO_2(02^00) + M\ (\tilde{\nu} = 1066\ cm^{-1}) + \Delta E = -3\ cm^{-1}$$

$$CO_2(00^01) + M(\tilde{\nu} = 286) = CO_2(10^00) + M\ (\tilde{\nu} = 1218\ cm^{-1}) + \Delta E = -29\ cm^{-1}$$

Since the transition multipole moments are not available for the indicated transitions, no attempt has been made to theoretically estimate the transition probabilities.

Carbon Dioxide - Iso-Propyl Alcohol:

The collisional energy transfer rates from $CO_2(00^0 1)$ to iso-propyl alcohol have been measured at 4 different temperatures in the range of 303 to 512°K. As in the case of CO_2 - normal-propyl alcohol, all the fluorescence signals exhibited single exponential decays. Hence the data reduction is identical to that of CO_2 n-propyl alcohol. A typical fluorescence decay curve (X_M = 0.02, P = 12,9 Torr, T = 439°K) is shown in Figure 8. In Figure 9, the fluorescence signal intensity is plotted against time on a semi-logarithamic plot, the slope of which yields τ^{-1}. The experiment is repeated for the same temperature and composition at different pressures of the mixture and in all cases τ^{-1} is estimated. Figure 10 shows the pressure dependence of τ^{-1}. It can be seen from the figure that only collisional deactivation is primarily responsible for the deactivation of $CO_2(00^0 1)$. The slope of this plot yields $(P\tau)^{-1}_{obs}$. A least square analysis of the data is performed to obtain $(P\tau)^{-1} = K_{obs}$. The studies are conducted with different compositions and the resulting K_{obs} values are plotted against X_M in Figure 11. A least square analysis of this data is carried out to obtain K_{CO_2-M}. The maximum composition of the mixtures for these studies is limited to 4 per cent of iso-propyl alcohol because of the fast rates which can be measured with the detector whose response time is approximately 3 μ sec. Such studies are repeated at 4 different temperatures in the range

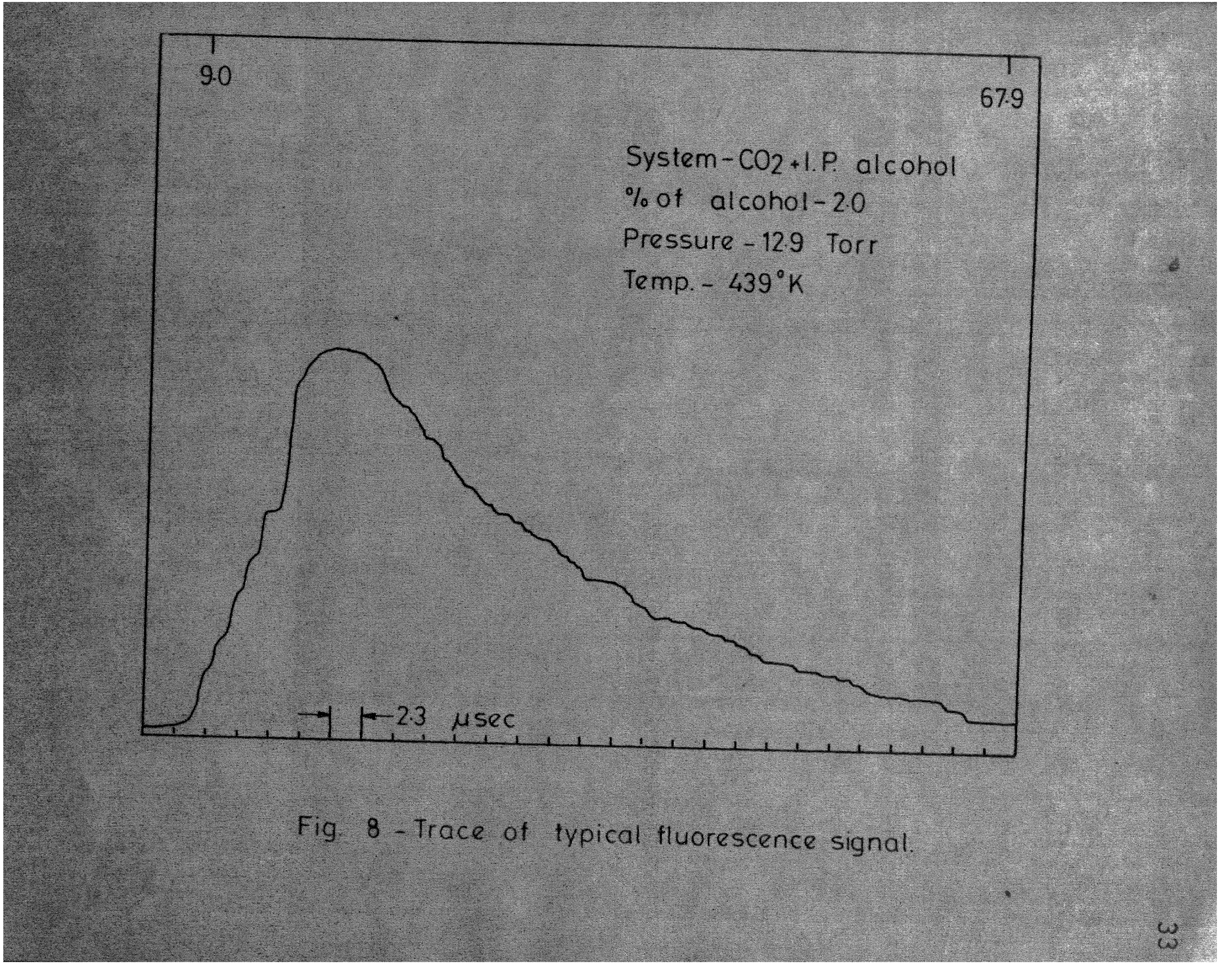

Fig. 8 - Trace of typical fluorescence signal.

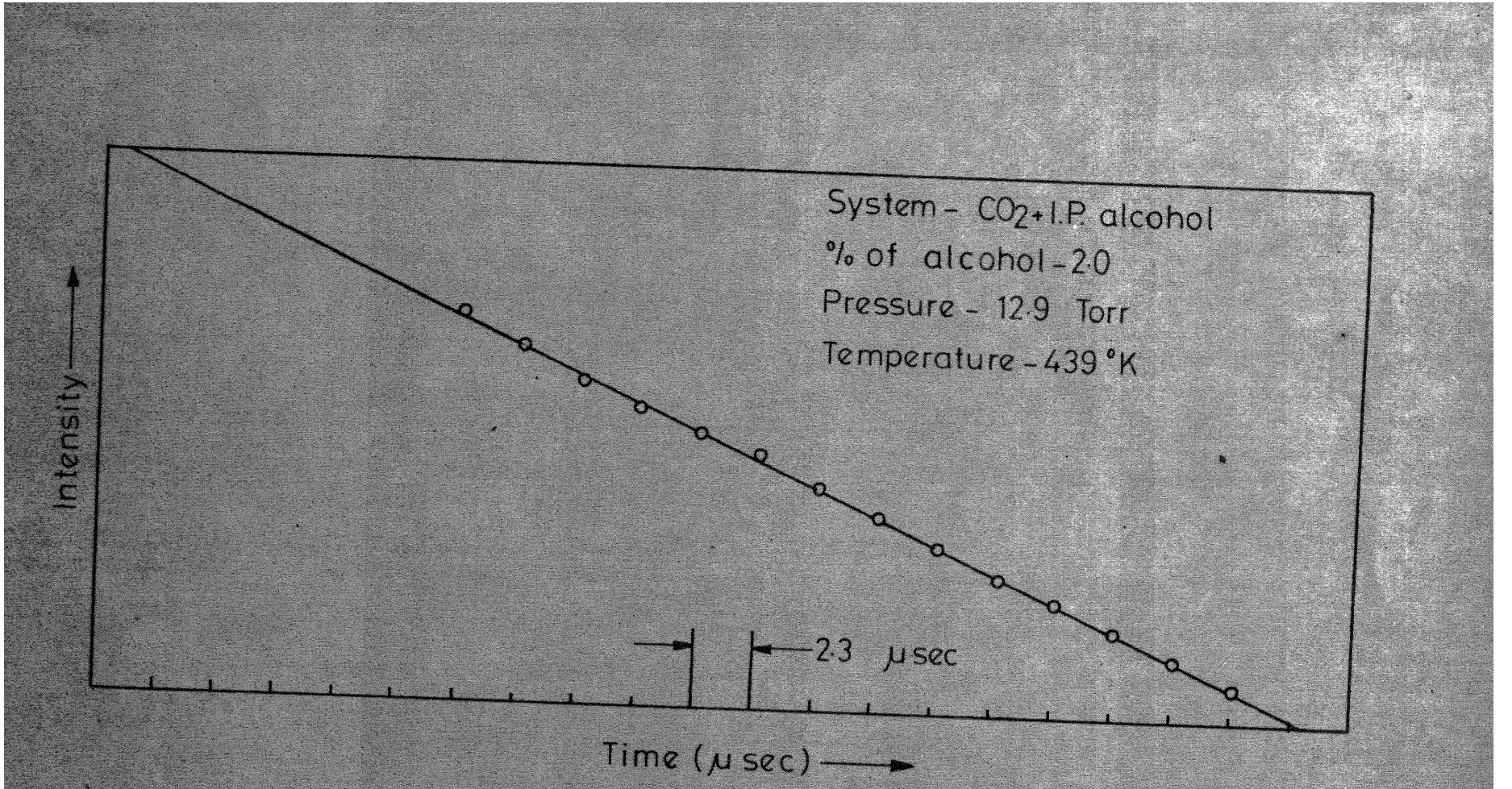

Fig. 9 -Semi-log plot of fluorescence decay curve.

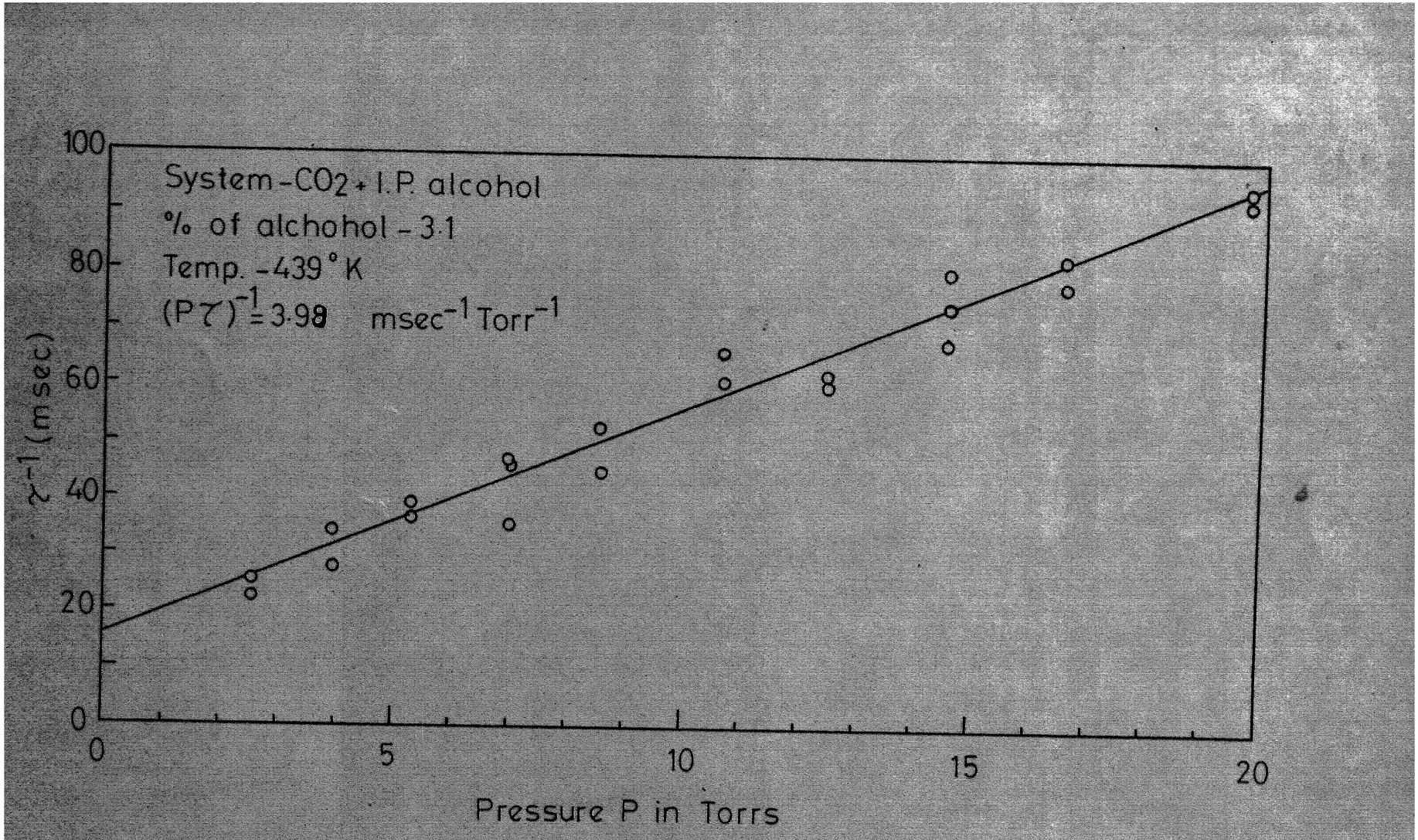

Fig. 10 - Plot of τ^{-1} vs. pressure.

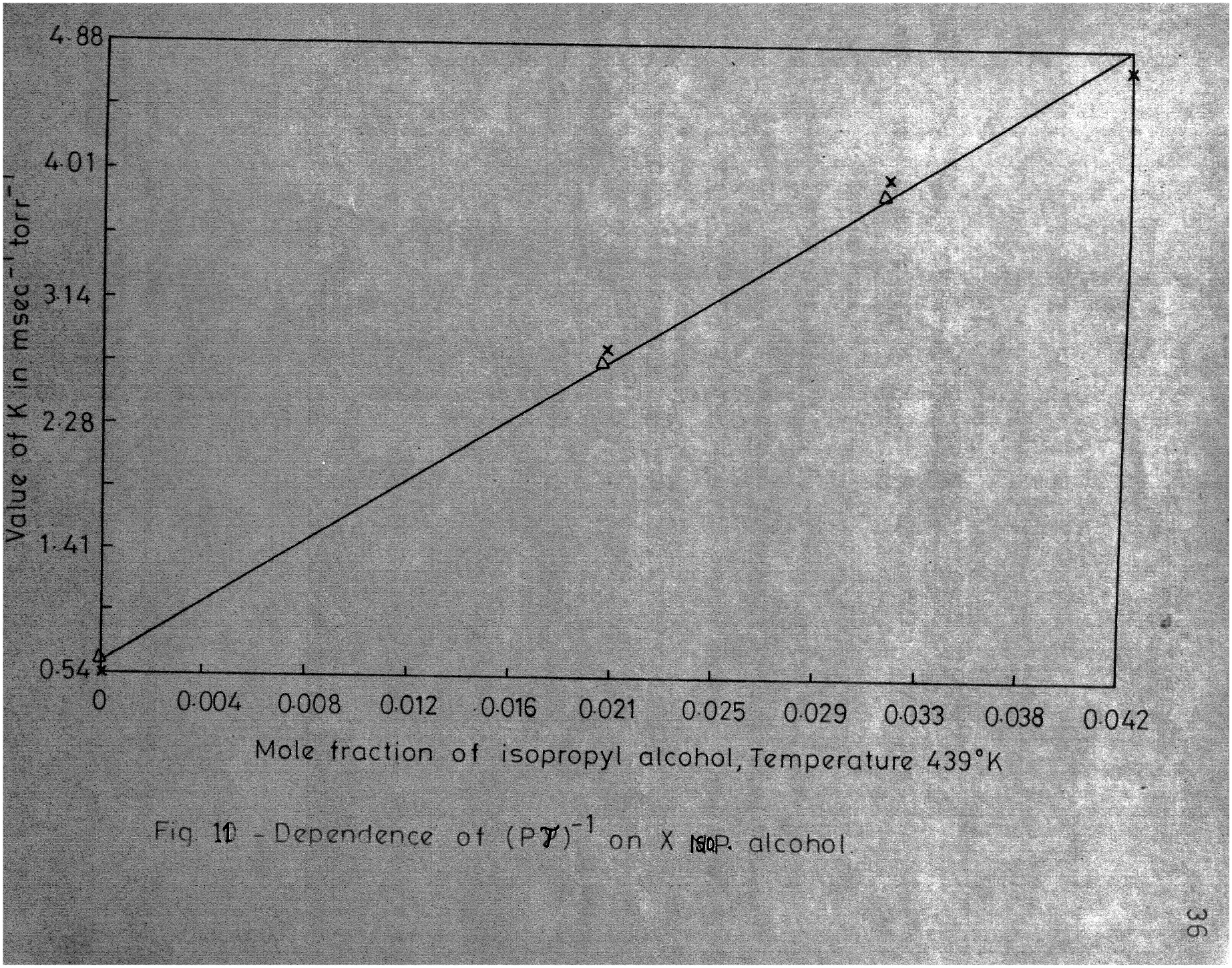

Fig. 11 - Dependence of $(PT)^{-1}$ on $X_{ISOP.}$ alcohol.

303 - 512°K. The temperature dependence of K_{CO_2-M} is shown in Figure 12 and the rest of the experimental results are presented in Tables 6-10.

The rate of deactivation of $CO_2(00^01)$ in collisions with iso-propyl alcohol is found to increase with decreasing temperature. Such temperature dependence and such high values of the deactivation rates suggest that long range forces could be responsible for energy transfer.

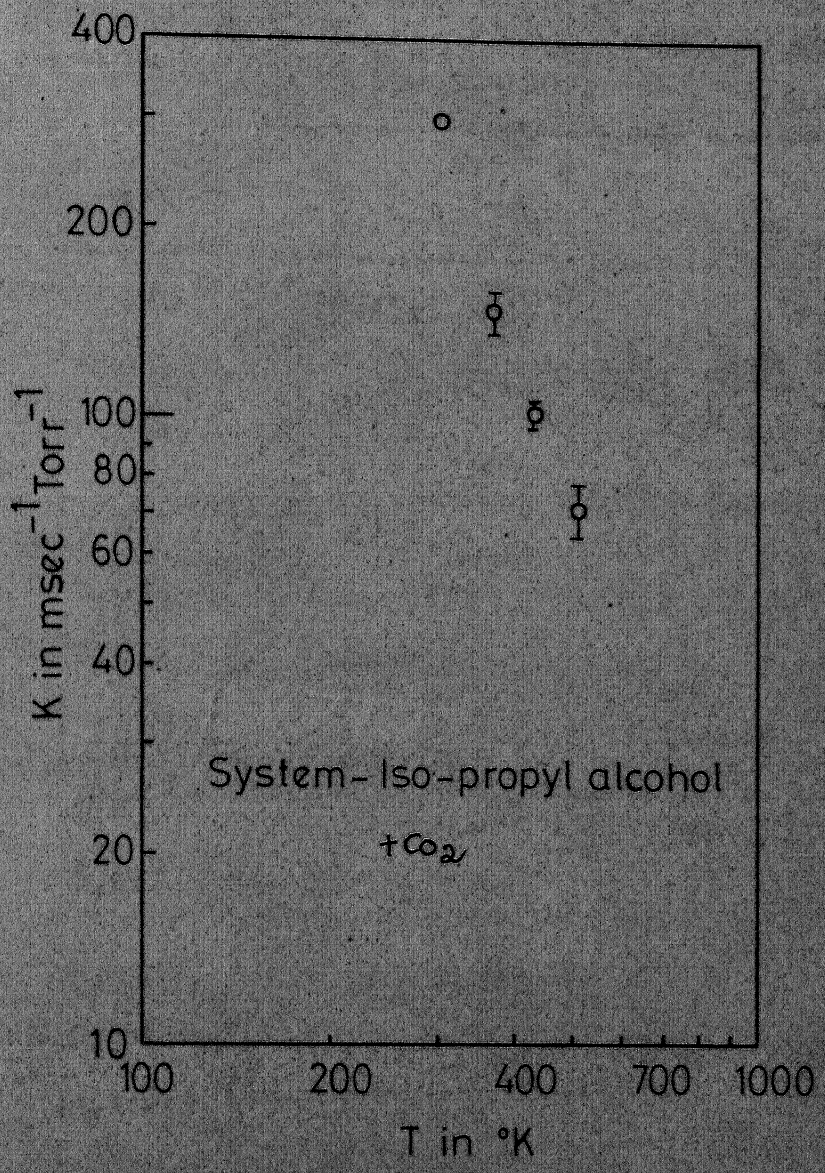

Fig. 12 -Temperature depenence of K.
(ln K vs ln T)

TABLE 6: RATE CONSTANTS AND CROSS-SECTIONS OF ENERGY TRANSFER FROM $CO_2(00^01)$ TO ISO-PROPYL ALCOHOL

Temp. in ^oK	Mole fraction of Iso-propyl alcohol	$(P\tau)^{-1}$ $msec^{-1}torr^{-1}$	K $sec^{-1}torr^{-1}$	σ^a $(\text{Å})^2$
303.0	0.021	$(6.45\pm1.26)^c$		
	0.032	-	293.64×10^3	1.850
	0.042	-		
373.0	0.021	3.87 ± 0.21		
	0.032	4.65 ± 0.32	$(147.29\pm11.25)\times10^3$	0.974
	0.042	6.92 ± 0.39		
439.0	0.021	2.8 ± 0.18		
	0.032	3.99 ± 0.16	$(100.72\pm3.32)\times10^3$	0.645
	0.042	4.75 ± 0.34		
512.0	0.021	2.54 ± 0.14		
	0.032	3.59 ± 0.18	$(71.09 \pm7.02)\times10^3$	0.581
	0.042	3.71 ± 0.21		

[a] The cross-sections σ are calculated according to eq.(2.2)

[c] The error limits correspond to 95 per cent confidence limits.

TABLE 7

Temperature = 512°K System: Carbon dioxide-iso-propyl alcohol
Pressure (P) in Torr; τ^{-1} in $msec^{-1}$; X-mole fraction of alcohol

X=0.042		X=0.032		X=0.021	
P	τ^{-1}	P	τ^{-1}	P	τ^{-1}
2.8	19.82	3.5	20.0	3.4	13.97
2.8	20.21	3.5	19.56	3.4	13.37
3.8	19.42	4.8	28.15	4.7	18.50
3.8	23.14	4.8	26.47	4.7	18.75
5.0	26.70	6.4	30.18	6.5	24.34
5.0	26.46	6.4	30.72	6.5	27.29
6.7	35.52	8.2	39.54	8.0	30.70
6.7	35.36	8.2	37.62	8.0	24.52
8.5	45.00	9.0	40.40	10.0	30.55
8.5	51.16	9.0	41.76	10.0	30.17
10.5	55.90	9.8	46.29	12.4	36.30
10.5	60.64	9.8	46.79	12.4	38.12
12.2	56.34	11.4	49.16	14.4	41.73
12.2	54.80	11.4	50.92	14.4	44.60
13.8	58.37	13.6	57.92	14.4	44.86
13.8	55.98	13.6	59.36	17.1	53.96
15.4	64.91	17.0	57.11	17.1	55.22
15.4	59.47	17.0	63.02	17.1	50.99
17.6	74.39	20.3	93.71	18.7	57.99
17.6	81.07	20.3	86.50	18.7	53.50
		20.3	75.90	18.7	51.36
		20.2	21.2	20.2	60.63
				20.2	46.21
$(P\tau)^{-1}=(3.71\pm0.22)$ $msec^{-1}Torr^{-1}$		$(P\tau)^{-1}=(3.59\pm0.18)$ $msec^{-1}Torr^{-1}$		$(P\tau)^{-1}=(2.54\pm0.14)$ $msec^{-1}Torr^{-1}$	

TABLE 8

Temperature: 439°K System: Carbon dioxide-iso-Propyl Alcohol
Pressure(P) in Torr; τ^{-1} $(msec)^{-1}$; X-mole fraction of alcohol

X=0.042		X=0.032		X=0.021	
P	τ^{-1}	P	τ^{-1}	P	τ^{-1}
2.0	19.47	2.6	22.31	2.5	15.66
2.0	19.07	2.6	25.08	2.5	13.18
2.7	22.99	3.9	27.77	4.3	32.98
2.7	23.92	3.9	34.13	4.3	21.81
3.8	38.60	5.3	36.66	5.8	27.42
3.8	30.80	5.3	39.00	5.8	26.06
5.2	44.94	7.0	46.46	7.2	39.14
5.2	37.10	7.0	45.63	7.2	35.27
6.9	55.22	7.0	34.86	8.9	50.80
6.9	53.80	8.6	52.59	8.9	44.18
6.9	67.67	8.6	44.56	8.9	42.04
8.4	47.74	10.6	60.77	10.7	38.80
8.4	57.07	10.6	64.97	10.7	44.19
10.0	65.17	12.5	62.24	13.0	47.06
10.0	71.07	12.5	60.06	13.0	50.41
10.0	77.09	14.6	74.01	15.9	57.16
11.7	65.02	14.6	68.15	15.9	58.13
11.7	58.15	14.6	79.99	18.4	60.51
11.7	72.70	16.6	77.95	18.4	66.94
13.6	75.23	16.6	82.83	20.1	70.18
13.6	74.29	19.8	92.80	20.1	68.70
15.2	83.59	19.8	94.71		
15.2	91.75				
$(P\tau)^{-1}=(4.75\pm0.34)$ $msec^{-1}Torr^{-1}$		$(P\tau)^{-1}=(3.99\pm0.16)$ $msec^{-1}Torr^{-1}$		$(P\tau)^{-1}=(2.80\pm0.18)$ $msec^{-1}Torr^{-1}$	

TABLE 9

Temperature=373°K

System: Carbon dioxide-iso-propyl alcohol

Pressure(P) in Torr; τ^{-1} in $msec^{-1}$; X-mole fraction of alcohol

X=0.042		X=0.032		X=0.021	
P	τ^{-1}	P	τ^{-1}	P	τ^{-1}
3.4	26.05	3.6	34.85	4.8	30.31
3.4	34.75	3.6	36.18	4.8	31.30
4.6	49.33	5.0	44.70	6.4	42.32
4.6	43,35	5.0	46.69	6.4	41.02
5.7	55.25	6.3	53.66	7.8	46.52
5.7	84.31	6.3	55.14	7.8	50.70
6.6	61.13	7.8	58.81	8.8	43.22
6.6	62.75	7.8	56.71	8.8	41.99
7.4	63.30	9.7	59.46	10.5	56.15
7.4	74.31	10.3	81.48	10.5	60.10
7.4	71.51	10.3	74.60	11.8	63.24
8.8	83.54	12.2	71.77	11.8	60.39
8.7	72.49	12.2	74.95	13.8	63.63
9.7	85.89	13.0	82.15	13.8	69.60
9.7	71.43	13.0	85.06	15.3	69.59
10.6	95.41	14.8	83.09	15.3	71.53
10.6	93.03	14.8	77.07	16.6	76.49
12.6	95.47	14.8	93.89	16.6	82.05
12.6	108.38	15.8	94.83	19.5	88.75
15.4	120.99	15.8	101.79	19.5	97.25
15.4	109.08	17.2	117.16		
		17.2	93.70		

$(P\tau)^{-1}=(6.92\pm0.30)$ $msec^{-1}Torr^{-1}$

$(P\tau)^{-1}=(4.65\pm0.32)$ $msec^{-1}$ $Torr^{-1}$

$(P\tau)^{-1}=(3.87\pm0.21)$ $msec^{-1}$ $Torr^{-1}$

TABLE 10

Temperature: 303°K System: Carbon dioxide-iso-propyl alcohol

Pressure (P) in Torr; $(\tau)^{-1}$ in $msec^{-1}$; X-mole fraction of alcohol

X = 0.021	
P	τ^{-1}
5.8	26.73
5.8	33.95
5.8	38.04
6.3	38.66
6.3	38.58
7.4	51.57
7.4	105.34
8.2	51.52
8.2	59.01
8.8	57.72
8.8	62.12
9.5	66.43
9.5	60.26
10.3	66.91
10.3	68.13
11.1	92.67
11.1	87.43
12.1	80.70
12.1	75.18
13.0	78.03
13.0	84.41

$(P\tau)^{-1} = (6.45 \pm 1.26)\ msec^{-1} Torr^{-1}$

CHAPTER 5

CONCLUSIONS

The V-V energy transfer rates in CO_2-propyl alcohol mixtures have been studied in the temperature range 303-514°K. The deactivation rates are found to decrease with increasing temperature. The large values of the energy transfer rates and their decrease with increasing temperature suggests that long-range multipole interactions are primarily responsible for the deactivation of $CO_2(00^0 1)$ mode. Since the energy levels of propyl alcohols are very close, several reaction paths may contribute towards the observed energy transfer rates.

It will be helpful if one can estimate energy transfer probabilities theoretically based on long-range multipole interactions and compare with the experimental data. If it is possible to follow the fluorescence from other levels, attempts should be made to study the various energy transfer processes and to plot the energy transfer map.

—

REFERENCES

1. Moeller, G. and Rigden, J.D., Applied Physics Letters 7, 274 (1965).
2. Moore, C.B., Wood, R.E., Hu, BEI-LOK, and Yardly, J.T., J. Chem. Phys. 46, 4222 (1967).
3. Patel, C.K.N., Phys. Rev. Lett., 12, 588 (1964).
4. Robinson, P.J., and Halbrook, K.A., 'Unimolecular Reactions', Wiley New York (1972).
5. C. Bradly Moore, 'Fluorescence (Chapter 3)' edited by Guilbault, Marcel Dekker, Inc., New York (1967).
6. B.A. Lengyl, Introduction to Laser Physics, Wiley, 1966.
7. L. Landau and E.Teller, Z. Phys. Sowjetunion 10, 34 (1936).
8. R.N.Schwartz, Z.I. Slawsky and K.F. Herzfeld, J.Chem. Phys. 20, 1591 (1952).
9. R.D. Sharma and C.A. Brau, J.Chem. Phys., 50, No.2, 15th Jan. (1969).
10. R.D. Sharma and C.A. Brau, Phys. Rev. Letters 19, 1273(1967).
11. Y.V. Chalapati Rao, Ph.D. Thesis (1972), IIT-Kanpur, India, Y.V. Chalapati Rao, V. Subba Rao and D. Ramachandra Rao, Chem. Phys. Letters, 17, 531 (1972).
12. W.A. Rosser, Jr., A.O. Wood and E.T. Gerry - J.C.P. 48, 4790 (1968).
13. J.C. Stephenson, and C.B. Moore - J.C.P., 56, 1295 (1972).
14. E.K. Plyler, J. Research, NBS, 48, 281, (1952).